

Charge-Density-Wave Order in 2H-NbSe₂

S. Koley,^{1,*} N. Mohanta,¹ and A. Taraphder^{1,2,†}

¹*Department of Physics, Indian Institute of Technology Kharagpur, W.B. 721302, India*

²*Centre for Theoretical Studies, Indian Institute of Technology Kharagpur, W.B. 721302, India*

Competition between collective states like charge density wave and superconductivity is played out in some of the transition metal dichalcogenides unencumbered by the spin degrees of freedom. Although 2H-NbSe₂ has received much less attention than some of the other members of the family (like 1T-TiSe₂ and 2H-TaSe₂), it shows superconductivity at 7.2 K and incommensurate charge ordering at 33 K. Recent experiments, notably Angle Resolved Photoemission spectroscopy, have cast serious doubts on the mechanism of Fermi surface nesting via electron-phonon interaction. The normal state has been found to be a poor, incoherent metal and remarkably, the coherence increases in the broken symmetry state. From a preformed excitonic liquid scenario, we show that there exists a natural understanding of the experimental data on 2H-NbSe₂ based on electron-electron interaction. The collective instabilities, in this scenario, are viewed as a condensation of an incoherent excitonic liquid already present at high temperature.

PACS numbers: 71.45.Lr, 71.30.+h, 75.50.Cc

I. INTRODUCTION

Strongly correlated electronic systems are one of the most studied materials in physics owing to their complexity and the competition between various ground states. A well-known example of this is the competition between charge density wave (CDW) and superconductivity in layered transition metal dichalcogenides (TMD) brought back to focus recently by a number of experiments^{1,2} (see Beck, et al.,³ for a recent review). The CDW in these systems was thought to be occurring via Peierls⁴ mechanism of a divergence in the response function in systems with Fermi surface (FS) nesting. Despite experimental and theoretical efforts, understanding CDW and related physical responses of a two dimensional layered TMD remains questionable for thirty years now. Recent discovery of superconductivity on intercalation and under pressure has rekindled the interest in them. Presence of unfilled or partially filled *d* band and an almost filled *p* band near Fermi level, with intra and inter-band interaction on a triangular lattice, produce competing broken symmetry states. A detailed understanding of these broken symmetry states in quantum matter is, therefore, at the heart of an understanding of the TMD as well⁵.

2H-NbSe₂ is one of the first 2D CDW systems known⁶, becomes a superconductor at 7.2 K and was, in fact, considered a "high *T_c* superconductor" prior to the cuprate-revolution. Even after about forty years, the mechanism of CDW in this system remains shrouded in mystery^{2,7-9}. In contrast to another, similar, 2H-type dichalcogenide, 2H-TaSe₂, which has a continuous transition from a normal to an incommensurate CDW state at 122 K and then a first order lock-in transition to a commensurate phase at 90 K, NbSe₂ has a second order phase transition from the normal to only a single CDW state at *T_{CDW}*=33 K. This ordered state finally shows superconductivity below 7 K. The search for Fermi surface (FS) nesting in the CDW transition of NbSe₂ has been a very strenuous one⁷, never showing any strong indication of nest-

ing at FS^{8,10} or saddle bands with appreciable density of states (DOS)^{8,11}. Moreover the charge susceptibility calculation shows no sharp peak at the CDW wave vector, *q_{CDW}* = (2 π /3, 2 π /3)^{9,10}. Though it has a broad peak in its real part, there is no discernible signature of the peak in the imaginary part⁹. In addition, it is found from angle resolved photoemission spectroscopy (ARPES) studies that FS is gapped only in certain directions^{8,10} and in the temperature-dependent charge excitation spectra, there is no indication of the opening of a gap, although the possibility of a pseudogap has been noted in ARPES, X-Ray and STM studies recently¹⁵. Consequently, there is no pronounced effect of CDW transition in the transport in 2H-NbSe₂², apart from a peak developing below *T_{CDW}*. As in 2H-TaSe₂, the in-plane resistivity of 2H-NbSe₂ is monotonic and approximately linear in *T* over a wide range of temperatures. The *c*-axis resistivity has almost similar *T*-dependence as the in-plane one, though the *c*-axis resistivity is much larger. The anisotropy, $\rho_c(T)/\rho_{ab}(T)$, is around 30 between 300 K and 100 K and decreases to about 10 at 10 K. $\rho(T)$ of 2H-NbSe₂ shows only a weak change of slope at the CDW transition at 33 K, below which an increased metallicity has been observed.

The optical conductivity shows a Drude peak and the typical 'shoulder-like' mid-infrared feature of a correlated system at about 300 K. Several differences between the two 2H dichalcogenides, 2H-NbSe₂ and 2H-TaSe₂, can be noticed in the scattering rate data also. The temperature dependence of the in-plane scattering rate in 2H-NbSe₂ is weak. Quite remarkably, the peak in the self-energy in the ARPES excitation spectra is located at different places at different energies, indicating a weak momentum dependence of self-energy in 2H-NbSe₂, coming, presumably, from electron-phonon coupling¹⁸. Contrast this to 2H-TaSe₂, where the peak in the self energy is at a range high enough for electron phonon coupling. Moreover, neutron¹² and x-ray scattering¹³ phonon dispersion data show a softening close to the CDW wave

vector in 2H-NbSe₂, lending credence to the coupling of phonons in the CDW transition of 2H-NbSe₂. The electron-phonon interaction being relevant here, may also cause the superconductivity to appear at a ‘higher’ temperature of around 7 K in this system, while superconductivity is found only at 200 mK in 2H-TaSe₂, where electron-phonon interaction is insignificant^{5,18}. Additionally, CDW transition does not affect the optical conductivity either, the zero energy Drude-like peak and its narrowing with decreasing temperature is a generic feature of 2D dichalcogenides.

All this indicates the formation of a pseudogap at a temperature above T_{CDW} as revealed in the recent experiments¹⁵ in 2H-NbSe₂ and theoretical analysis of TMD⁵. The progressive narrowing of the Drude peak in the far infrared region on lowering the temperature coexists with mid-infrared absorption. Considering all, these results point to the inadequacy of the FS nesting scenario based on LDA studies. If FS nesting were in operation, then FS and transport data would show opening of a CDW gap at the reconstructed FS and a severe drop in conductivity entering in to the commensurate CDW state, which are in conflict with available experimental results. Besides, the band picture cannot be reconciled with the temperature dependent large spectral weight transfer (SWT) observed. A theory should fulfil all these criteria and describe the smooth crossover of the normal state to a CDW phase. A preformed excitonic liquid (PEL) scenario⁵, which successfully described 2H-TaSe₂ and 1T-TiSe₂ (with the addition of electron-lattice coupling in the latter) can resolve this if the PEL appears at high T . This can condense into a CDW state at low T via electron-lattice coupling.

II. METHOD

We propose a preformed excitonic liquid scenario for 2H-NbSe₂ and show that a wide range of normal state properties could be understood within this picture. We use exciton-phonon coupling for the emergence of an unconventional CDW state at lower T as instabilities of an incoherent preformed excitonic liquid via exciton-lattice interaction.

The tight binding band structure of 2H-NbSe₂ was constructed from a 22×22 matrix using Nb- d and Se- p states. We show the two bands closest to E_F (with predominantly Nb- d_{z^2} and Se- p_z character) in top left inset of Fig. 1, as well as the FS (top right inset) and the DOS (main panel), in fairly good agreement with LAPW results¹⁴. Only one, nearly spherical, FS sheet can be seen in the LDA FS (Fig. 1 right inset) which is already in contradiction with the notion of FS nesting for CDW formation. In the TMD systems the conduction d -band is nominally either half-filled or empty and the valance band is nominally filled. The LDA shows partially filled conduction and valance bands with low carrier density. In this situation, the formation of exciton comes about via a

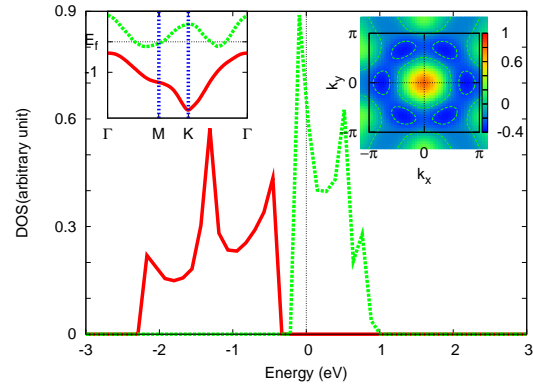


FIG. 1. (Color Online) Non interacting DOS (main panel), bands closest to FL (left inset) and Fermi surface (right inset) calculated from a tight binding fit (see text). The red band represents the band with predominantly Se- p character and the green band is predominantly of Nb- d character.

sizable $d_{z^2}-p_z$ mixing, which hybridises the electrons and holes in the d and p bands in conjunction with dynamical renormalization and electron-hole attraction by U_{ab} . Besides, at finite temperatures, there are thermally generated holes in the valence band aiding the excitonic instability. In this situation a small electron correlation will form excitons at high T . The electronically active states comprise Nb- d_{z^2} and Se- p_z bands and $U \simeq 0.7$ eV and $U_{ab} \simeq 0.05$ eV are the typical values of interactions where exciton formation is found to be most likely. In view of the bad metallic normal state, the ordering instabilities of such bad metals *cannot*, by construction, be rationalised by appealing to static-mean-field theory: this can only be reliably accessed by approaches which capture dynamical correlations adequately. For 2H-NbSe₂, a minimal two-band correlated model as defined below is mandated by tight binding results, and adequate treatment of dynamical correlations underlying incoherent behavior is achieved by dynamical-mean field theory (DMFT). The DMFT is now proved to be one of the most successful approaches to correlated electronic systems, making them attractive tools to use in the present context. The two-band Hubbard model we use is ($d_{z^2} = a$ and $p_z = b$)

$$H_{el} = \sum_{\mathbf{k}, l, m, \sigma} (t_{\mathbf{k}}^{l \neq m} + \epsilon_l \delta_{lm}) c_{\mathbf{k}l\sigma}^\dagger c_{\mathbf{k}m\sigma} + U \sum_{i, \mu} n_{i\mu\uparrow} n_{i\mu\downarrow} + U_{ab} \sum_i n_{ia} n_{ib} \quad (1)$$

where l, m , take values a, b and U is the intra-orbital Coulomb correlation (taken to be same for a, b being small compared to band-width (see later); we have checked that results are insensitive to this choice within reasonable limits); U_{ab} is the inter-orbital correlation. Further, in TMD, the most relevant A_{1g} phonon mode

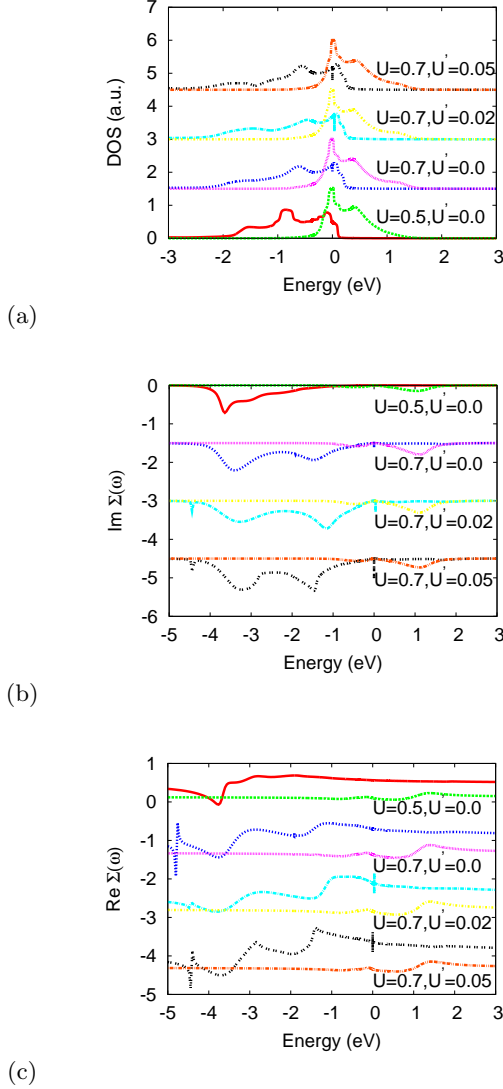


FIG. 2. (Color Online) DMFT (a) DOS of Nb-*d* band and Se-*p* band for several U and U' ($=U_{ab}$). The DOS with peak near FL is from Nb-*d* band. (b) Imaginary and (c) real part of self energy for the same values of U and U' as in (a). The self energies with a dip-like structure close to -1 eV in the imaginary part are the *p* band self-energies.

couples to the inter-band excitons by symmetry, and the electron-phonon coupling is $H_{el-l} = g \sum_i (A_i + A_i^\dagger)(c_{ia}^\dagger c_{ib} + h.c.)$. To solve $H = H_{el} + H_{el-l}$ within DMFT, we have combined the multi-orbital iterated perturbation theory (MOIPT) for H_{el} ¹⁶ with the DMFT for polarons by Ciuchi *et al.*¹⁷. Finally, we address the broken symmetry phase quite differently⁵ from the LDA based pictures involving band folding. This is called for, from the above discussions and LCAO+DMFT results below, since the ‘normal’ state is found to be an incoherent PEL at high temperature without well defined Landau quasiparticles. Instability to CDW order then cannot occur via the tra-

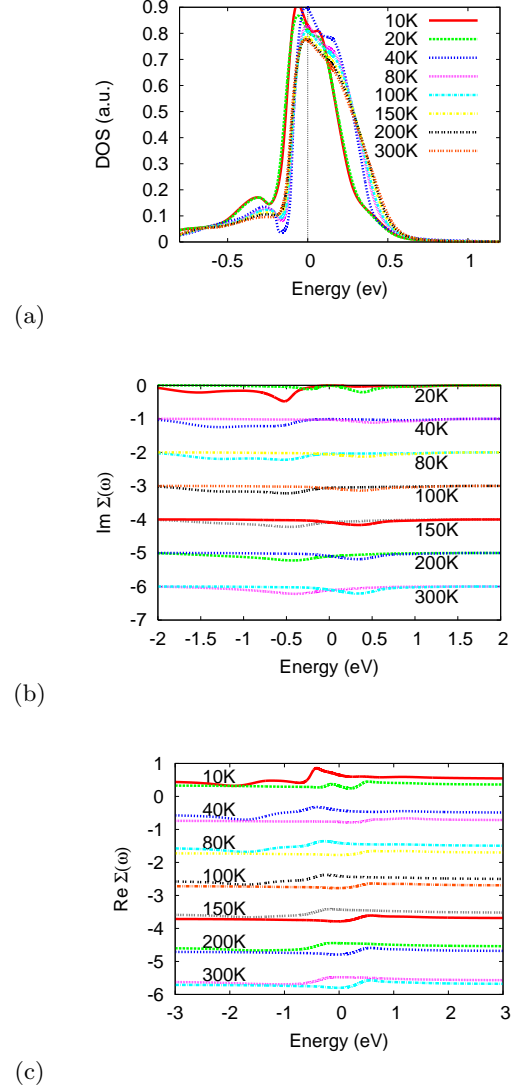


FIG. 3. (Color Online) Temperature evolution with $U = 0.5$ eV, $U_{ab} = 0.05$ eV, $t_{ab} = 0.1$ eV and phonon coupling 0.05 eV of (a) DOS of Nb-*d* band. (b) Imaginary and (c) real part of self-energy of *p* and *d* band. The self-energies with a dip like structure close to -0.5 eV in the imaginary part are for Se-*p* band.

ditional band-folding involving Fermi liquid quasiparticles. Rather, since *coherent* one-particle inter-band mixing is inoperative, ordered states must now arise directly as two-particle instabilities of the bad metal. This is a situation reminiscent of 2H-TaSe₂⁵ and we employ similar arguments here. So for 2H-NbSe₂ as well, the two particle interaction is more relevant than the incoherent one-electron mixing and therefore we construct an effective Hamiltonian involving two-particle processes:

$H_{res} \simeq -t_{ab}^2 \chi_{ab}(0,0) \sum_{\langle i,j \rangle, \sigma, \sigma'} c_{ia\sigma}^\dagger c_{jb\sigma} c_{jba\sigma'}^\dagger c_{ia\sigma'}$, with χ_{ab} the inter-orbital susceptibility. Decoupling this intersite interaction in a generalised HF sense we will get two competing instabilities: $H_{res}^{(HF)} =$

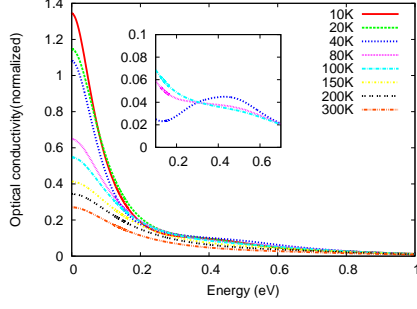


FIG. 4. (Color Online) Optical Conductivity at various temperature from DMFT. The same (inset) at low energy showing extended shoulder like feature in an enlarged scale.

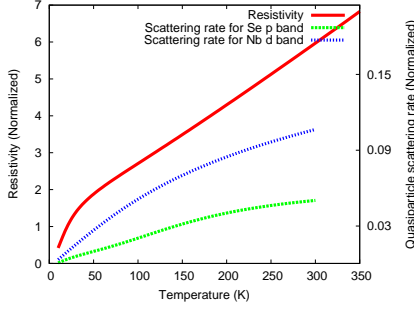


FIG. 5. (Color Online) Temperature dependent dc resistivity (left side scale) and scattering rates for the two bands (the scale on the right side).

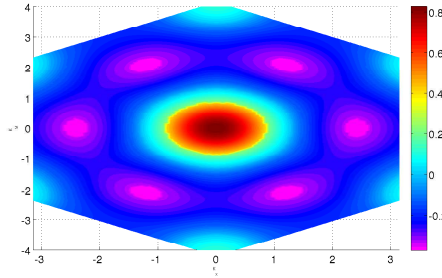
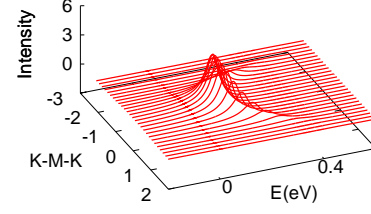
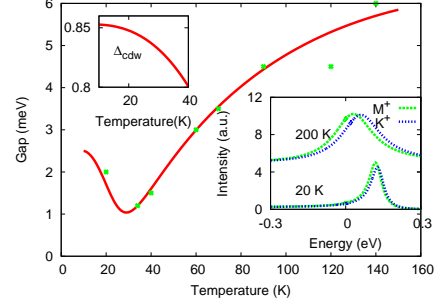


FIG. 6. (Color Online) The interacting Fermi surface at 20K.

$-\sum_{\langle i,j \rangle, \sigma\sigma'} (\Delta_{1b} c_{ia\sigma}^\dagger c_{ia\sigma} + \Delta_{ab} c_{ia\sigma}^\dagger c_{jb-\sigma}^\dagger + a \rightarrow b)$, with $\Delta_{cdw} = (\Delta_{1a} - \Delta_{1b}) \simeq \langle n_a - n_b \rangle$ representing a CDW and $\Delta_{ab} \simeq \langle c_{ia\sigma} c_{jb-\sigma} \rangle$ a multiband spin-singlet superconducting (SC) order parameters. In what follows, at low temperature, we only concentrate on the broken symmetry CDW phase. The singlet SC instability is an issue we will take up in the future. What is clear is that, owing to the characteristic form factor of the coefficient in the two-fermion term in the effective Hamiltonian, the SC order parameter is expected to be anisotropic. In the



(a)



(b)

FIG. 7. (Color Online) (a) Energy-momentum distribution of intensities along K-M-K high symmetry direction. (b) Variation of Gap (as defined by Borisenko et al.¹⁰) with temperature. The green dots are the experimental points¹⁰ for comparison. Inset of lower panel shows energy distribution curves (EDC) at 20 K and 200 K along K^+ and M^+ direction (again, as defined in Borisenko, et al.) The inset on top shows CDW amplitude with temperature.

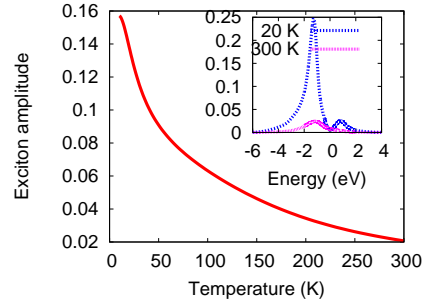


FIG. 8. (Color Online) Inter-orbital excitonic order parameter. Inset shows imaginary part of the off-diagonal Green's function at 20 K and 300 K.

low temperature phase, we ignore this unconventional SC order parameter and use the mean-field decoupling of the effective Hamiltonian in the particle-hole channel and calculate the order parameter and transport in the CDW phase at low T .

III. RESULTS

Going back to Hamiltonian Eq.(1) and following the standard multi-orbital DMFT procedure with iterated perturbation scheme²³ as the impurity solver⁵, we compute the DMFT spectral function and transport properties in the normal state. We first work out the case without electron-phonon coupling. We show how our theory describes the available data on 2H-NbSe₂ without further assumptions. As is well known, DMFT modifies LDA bands in two major ways: first, the static, Hartree terms renormalize the relative band positions (depending on the band occupations and their relative separation), and second, the dynamical correlations generically cause spectral weight transfer (SWT) across a fairly large energy scale dictated by correlation: indeed LDA fails in a major way to incorporate the physics of this and does not lead to SWT. We show the DMFT many-body DOS for Nb-d and Se-p bands in Fig. 2a and the corresponding imaginary and real parts of the self-energies in Fig. 2b and Fig. 2c with several U and U_{ab} ($t_{ab} = 0.1$ eV). The DOS is quite sensitive to the choice of U and U_{ab} . Application of small finite $U_{ab} = 0.05$ eV for $U = 0.7$ eV causes instability in the Se- p band at $\omega = 0$, implying an orbitally selective insulator with very poor conductivity (the d-band has a small but finite DOS at the FL). However, the real system remains metallic throughout, albeit a poor one, and therefore U and U_{ab} are chosen accordingly, $U = 0.5$ eV, $U_{ab} = 0.05$ eV, so that the system remains a poor metal.

However, the real system is known to show reasonable phonon coupling in its physical properties. The phonons do not appear to play any central role in the unusual normal state properties or the formation of CDW², they couple with the excitons and therefore the changes in phonon intensities and lineshape is a useful tool to shed light on the underlying physics in NbSe₂. Our DMFT results also indicate that the phonons are not responsible for the normal state properties (and even the CDW formation, see later), we include the phonons in our calculations in the following and study their evolution. In Fig. 3a we show the resulting many body DOS at high ($T > T_{cdw}$) and low $T (< T_{cdw})$ for the Nb-d band for $U=0.5$ eV and $U_{ab} = 0.05$ eV along with the self-energies for both the bands. Neglect of the mixing term t_{ab} in the Hamiltonian Eq.1 leads to results that strongly disagree with the extant experimental observations. Besides, the excitonic amplitude will vanish in the ground state for $t_{ab} = 0$. Inclusion of mixing produces a bad metallic state with a DOS having a peak-like structure at FL, which goes down as temperature rises. We also find $\text{Im}\Sigma_{a,b}(\omega = 0) > 0$ at E_F , underlining the incoherent normal properties observed. The p and d bands continue to show renormalized bad metallic behavior throughout the temperature range. Clearly, this is caused by the incoherent excitonic fluctuations present in the system already at high temperatures. Quite remarkably, the self-energy also indicates a large scattering rate at high T in the normal state, reducing as

T is lowered - an indication of the build up of excitonic coherence at lower T . The peak in self-energy varies in an energy range where phonons are known to be active (as seen by Valla et al.¹⁸).

If this alternative PEL-based theory is to be valid, then it should be able to describe more experimental observations. ARPES data show a gradual build-up of excitonic correlations with decreasing temperature as an increase in the pseudogap¹⁰. The pseudogap deepens and the low-energy peak in PES shifts out to higher energy, accompanied by temperature-induced spectral weight transfer from low to high energy. This is a real test for our theory. It is already clear that LDA plus static HF cannot explain the ARPES lineshapes and the spectral weight transfer. However, our formulation must also describe the unusual transport properties. In Fig. 4 we show our DMFT results for the T -dependent optical conductivity, $\sigma(\omega, T)$, calculated from the many body (DMFT) Green's function. Both the ω and T dependence of $\sigma(\omega, T)$ are in agreement with experiment. In $\sigma(\omega, T)$ a correlated FL behavior is never found and lowering of T shows a reduction in the incoherent scattering. At low T a shoulder-like feature is seen around 0.25 eV. This is exactly the scale at which a pseudogap feature appears in the T -dependent DOS at low T (shown in Fig. 3a), strongly suggesting the tendency of the preformed excitons towards coherence at lower T . Clearly this shoulder-like feature in optical conductivity disappears at high T due to incoherent excitonic effects. DMFT result for T dependent dc resistivity is shown in Fig. 5, which also agrees qualitatively with experimental data. The dc resistivity $\rho(T)$ is strongly dominated by the incoherent scattering leading to a non Fermi liquid behaviour (nFL); there is no T^2 regime at low T i.e., it never shows a correlated Fermi liquid behavior (quite similar to 2H-TaSe₂). The high temperature resistivity is linear in T for a large range of T as observed in the experiments. The scattering rates (5) track the resistivity and are almost linear at high T , getting reduced as T decreases as in the experimental data². $\rho(T)$ shows a change in slope at around 30 K, below which enhanced metallicity is recovered. We reconcile this bump in resistivity as coming from the enhanced coherence of preformed excitons below a crossover temperature range causing reduced incoherent scattering. The preformed excitons eventually condense to a CDW at low temperature (see below). This picture therefore naturally reconciles with the near-insensitivity of the transport data to the onset of the commensurate CDW order and enhanced metallicity below it.

The detailed FS map as a function of T in NbSe₂ does not show a strong signature of FS nesting. The DMFT FS can be approximately constructed from the DMFT Green's function²⁰. FS map at lower temperature, shown in Fig. 6 in the original unreconstructed Brillouin zone, clearly shows that the *correlated* FS is not affected significantly across the CDW transition. The Fermi pockets are visible at $T > T_{CDW}$, albeit with a typical scatter coming from incoherent scattering and consequent loss

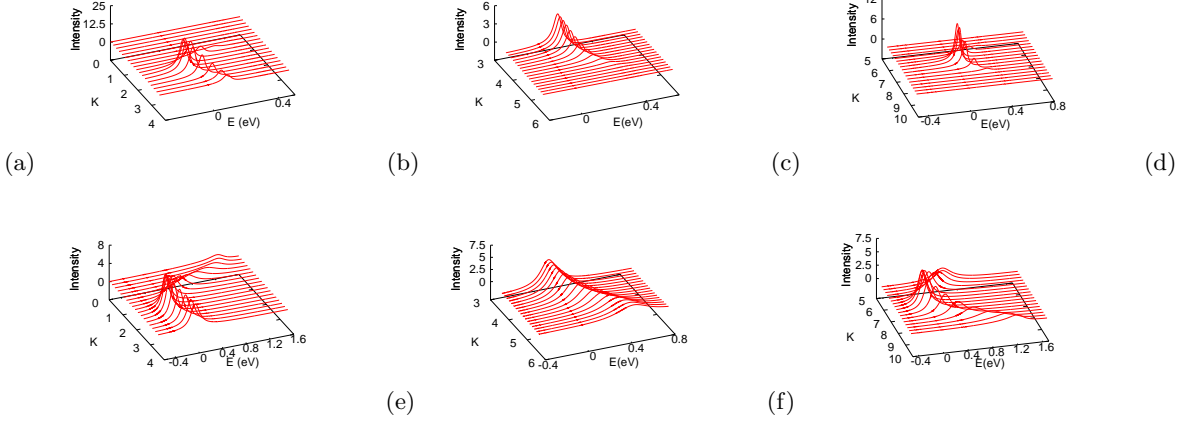


FIG. 9. (Color Online) Calculated ARPES spectra along (i) Γ -M (ii) M-K and (iii) K- Γ direction at 20 K (a-c) and 200 K (d-f). $E = 0$ marks the Fermi level.

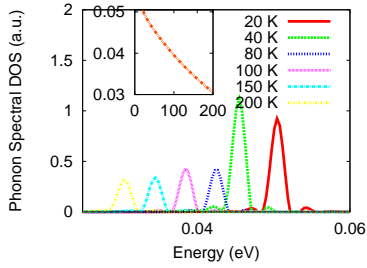


FIG. 10. (Color Online) Phonon spectral density at different temperatures. The inset shows the peak positions with temperature in the normal state.

of quasiparticle feature. This loss of sharpness correlates well with the broadness of lineshape (Fig. 3) and spectral weight transfer from incoherent scattering. Across $T = T_{CDW}$ there is no dramatic change: since excitons are formed at higher temperatures and parts of the FS have already been reconstructed at high T , changes in FS at the CDW transition is therefore small. This is of course corroborated by the transport data as well. The normal state is thus dominated by incoherent scattering and the onset of CDW order eventually involves condensation of these preformed excitons. Finally, given the in-plane normal state is incoherent, the out-of-plane responses will show even more drastic signatures of incoherence¹⁹. This is borne out in the optical conductivity measurements² for 2H-NbSe₂. Thus, the preformed-excitonic liquid scenario provides a natural basis to understand a wide variety of responses in the normal state of 2H-NbSe₂.

Since there is no prominent or discernible gap in the FS at the CDW transition, Borisenko et al¹⁰. have defined a “gap” as the difference between the binding energies of the leading-edge midpoints. This gap is observed in the

normal state also and is, in fact, much larger than the gap at the CDW transition. Theoretical ARPES lineshapes along K-M-K direction and the gap are shown in Fig. 7 for comparison. Evidently the theoretical gap structure tracks the experimental one fairly well as shown in Fig. 7b. The gap for temperatures below T_{CDW} is higher than the gap near T_{CDW} Fig. 7b, suggesting, in fact, a minimum gap at the transition temperature. The CDW transition temperature can thus be defined as the temperature where the gap between the leading edge midpoints is a minimum. The CDW order parameter obtained from the effective Hamiltonian, is also plotted in the inset to Fig. 7b and it has the characteristic decrease with temperature, although not following the static single-particle mean-field square-root variation.

The evolution of the exciton-phonon correlation with temperature can be seen through the excitonic spectral function $\rho_{ab}(\omega) = (-1/\pi)\text{Im}G_{ab}(\omega)$ as well as the local excitonic average, $\langle(c_{ia\sigma}^\dagger c_{ib\sigma} + h.c.)\rangle = (-1/\pi)\int_{-\infty}^{\infty} d\omega \text{Im}G_{ab}(\omega)$ in Fig. 8. The strong temperature-dependence of $\rho_{ab}(\omega)$ is obvious: at high T , the broad, asymmetric shape is a manifestation of the incoherent excitonic fluid, while the low-energy pseudogap along with large spectral weight transfer with decreasing T signals a progressive build-up of incipient excitonic coherence. This is seen more clearly in the T -dependence of $\langle(c_{ia\sigma}^\dagger c_{ib\sigma} + h.c.)\rangle$, where a relatively steep increase below 30 K is visible (Fig. 8), while the fluctuations are present till fairly high temperatures. Remarkably, this exactly correlates with the broad bump in $\rho(T)$ in Fig. 5 and is a clear evidence for the relevance of strong, dynamic excitonic correlations in 2H-NbSe₂. A regime of strong pair-fluctuation above T_{cdw} and the existence of a pseudogap far in to the normal state where there is no long range order, has been seen in the X-ray, ARPES and tunnelling spectroscopy in NbSe₂ recently¹⁵. Our results are indeed quite consistent with such observations. Theoretical ARPES lineshapes along high sym-

metry directions in Fig. 9 mark exciton-phonon-induced changes in the k -resolved spectrum at normal state and in the CDW phase. The ARPES dispersions match quite well with the observed spectra and present how the incoherent high-temperature normal state is going over to a progressively coherent ordered state, establishing the exciton-phonon scenario on a stronger footing. Given the form of exciton-phonon coupling, by symmetry, the resulting DMFT phonon spectrum (Fig. 10) should show particular changes going hand in hand with exciton dynamics. The DMFT phonon spectrum of NbSe₂ shows maximum intensity with reduced linewidth in the CDW phase. Broadening of phonon spectrum above T_{CDW} confirm coupling with incoherent excitons at high T . As T is lowered below T_{CDW} the onset of excitonic coherence reduces normal state scattering, resulting in sharpening of the phonon spectrum. In the light of our results, it is quite likely that the instability of the incoherent metal to an UCDW state at low T in 2H-NbSe₂ results from a mechanism where the one-electron process is incoherent while the electronic correlations as well as the interactions mediated by exciton-lattice coupling are relevant. Superconductivity in other TMD arises from an incoherent metal, in most cases proximate to CDW states, which is likely to be the case here too. Such a scenario appears to be generic for all the three TMDs we have studied^{5,22} and may be applied to other TMDs also. Our approach stresses on the central role of dynam-

ical excitonic correlations in small carrier density systems having close-by electron- and hole-like bands at E_F . We believe that approaches similar to the one presented here and the similarity of the underlying physics with other TMD systems studied earlier^{5,21,22} underline a common theme of PEL in the normal state and its condensation at the CDW transition.

With the recent advances in the ultrafast spectroscopy and its application to ordered electronic states^{24,25}, it may indeed be possible to resolve the issue of a correlation-driven versus phonon-driven mechanism for CDW in many systems owing to the two different time-scales associated with the two processes. The resolution of 1T-TiSe₂ as an electronically driven excitonic mechanism²⁴ lends credence to the fact that the PEL mechanism may be operative in other TMD systems too^{5,22}. Electronic Raman spectroscopy and the determination of the nature and symmetry of the low temperature superconducting states remain other experimental observations that would shed light on these systems and test the proposed theories.

SK acknowledges CSIR (India) for financial support through a senior research fellowship. AT and SK acknowledge useful discussion and close collaboration on similar systems with Mukul Laad and N S Vidhyadhiraja. AT acknowledges useful discussions with and inputs from Chong-Yu Ruan on possible pump probe experiment.

-
- * skoley@phy.iitkgp.ernet.in
† arghya@phy.iitkgp.ernet.in
- ¹ C. Monney, et al., Phys. Rev. B **81**, 155104 (2010).
 - ² S. V. Dordevic, et al., Eur. Phys. J. B **33**, 15 (2003).
 - ³ C. Monney et al., New Journal of Physics **12**, 125019 (2010).
 - ⁴ R. E. Peierls, *Quantum Theory of Solids* (Clarendon, Oxford, 1955).
 - ⁵ A. Taraphder et al., Phys. Rev. Lett **106**, 236405 (2011).
 - ⁶ J A Wilson, et al., Adv. Phys. **24**, 117 (1975).
 - ⁷ Th. Straub, et al., Phys. Rev. Lett. **82**, 4504 (1999).
 - ⁸ D. W. Shen, et al., Phys. Rev. Lett. **101**, 226406 (2008).
 - ⁹ M. D. Johannes and I.I. Mazin, Phys. Rev. B **77**, 165135 (2008).
 - ¹⁰ S. V. Borisenko et al., Phys. Rev. Lett **102**, 166402 (2009).
 - ¹¹ W. C. Tonjes, et al., Phys. Rev. B, **63**, 235101 (2001).
 - ¹² D. E. Moncton et al., Phys. Rev. Lett **34**, 734 (1975); Phys. Rev. B **16**, 801 (1977).
 - ¹³ B. M. Murphy et al., Phys. Rev. Lett **95**, 256104 (2005); J. Phys. Condens. Matter **20**, 224001 (2008).
 - ¹⁴ N. J. Doran et al., J. Phys. C: Solid State Phys. **11**, 685 (1978).
 - ¹⁵ U. Chatterjee, et al., unpublished and private communication.
 - ¹⁶ M. Laad, et al., Phys. Rev. Lett. **91**, 156402 (2003).
 - ¹⁷ S. Ciuchi et al., Europhys. Lett. **30**, 151 (1995).
 - ¹⁸ T. Valla et al., Phys. Rev. Lett **92**, 086401 (2004).
 - ¹⁹ P. W. Anderson, (1997) (Princeton University Press).
 - ²⁰ K Byczuk et al., Nat. Phys. **3**, 168 (2007).
 - ²¹ S Koley et al., AIP Conf.Proc. **1461**, 170 (2012).
 - ²² S Koley et al., arXiv:1212.1026.
 - ²³ Iterated Perturbation scheme has been very successfully used in several cases, see for example, V. I. Anisimov, et al. Jour. Phys. Cond. Mat, **9**, 7359 (1997) and M. Laad, et al.¹⁶.
 - ²⁴ S. Hellmann, et al, Nature Comm.**3**, 1069 (2012).
 - ²⁵ Tzong-Ru T. Han, et al, Phys. Rev. B **86**, 075145 (2012).